HHS Public Access

Author manuscript

J Atheroscler Thromb. Author manuscript; available in PMC 2017 July 13.

Published in final edited form as:

J Atheroscler Thromb. 2015 August 26; 22(8): 833–844. doi:10.5551/jat.27292.

Angiotensin II Activates MCP-1 and Induces Cardiac Hypertrophy and Dysfunction via Toll-like Receptor 4

Susumu Matsuda[1], **Seiji Umemoto**[2], **Koichi Yoshimura**[3], **Shinichi Itoh**[1], **Tomoaki Murata**[4], **Tohru Fukai**[5], and **Masunori Matsuzaki**[1]

[1]Department of Medicine and Clinical Science, Yamaguchi University Graduate School of Medicine, Yamaguchi, Japan

[2]Center for Clinical Research, Yamaguchi University Hospital, Yamaguchi, Japan

[3]Department of Surgery and Clinical Science, Yamaguchi University Graduate School of Medicine, Yamaguchi, Japan

[4]Institute of Experimental Animals, Science Research Center, Yamaguchi University, Yamaguchi, Japan

[5]Departments of Medicine (Section of Cardiology) and Pharmacology, Center for Cardiovascular Research, University of Illinois at Chicago, Chicago, IL, USA

Abstract

Aim—Angiotensin II (AngII) produces reactive oxygen species (ROS), thus contributing to the development of cardiac hypertrophy and subsequent heart failure, and stimulates the expression of monocyte chemoattractant protein-1 (MCP-1). In addition, Toll-like receptor 4 (TLR4) is involved in the upregulation of MCP-1. In order to clarify whether TLR4 is involved in the onset of cardiac dysfunction caused by AngII stimulation, we investigated the effects of TLR4 on oxidative stress, the MCP-1 expression and cardiac dysfunction in mice with AngII-induced hypertension.

Methods—TLR4-deficient ($Tlr4^{lPS\text{-}d}$) and wild-type (WT) mice were randomized into groups treated with AngII, norepinephrine (NE) or a subdepressor dose of the AngII receptor blocker irbesartan (IRB) and Angll for two weeks.

Results—AngII and NE similarly increased systolic blood pressure in all drug-treated groups compared to that observed in the control group among both WT and $T1r4^{lps\text{-}d}$ mice ($p< 0.05$). In the WT mice, AngII induced cardiac hypertrophy as well as vascular remodeling and perivascular fibrosis of the intramyocardial arteries and monocyte/macrophage infiltration in the heart ($P<0.05$). Furthermore, AngII treatment decreased the left ventricular diastolic function and resulted in a greater left ventricular end-systolic dimension ($P<0.05$) in addition to producing a five-fold increase in the NADPH oxidase activity, ROS content and MCP-1 expression ($P<0.05$). In contrast, the $Tlr4^{lps\text{-}d}$ mice showed little effects of AngII on these indices. In the WT mice, IRB

Address for correspondence: Seiji Umemoto, Center for Clinical, Research, Yamaguchi University Hospital, 1-1-1 Minami, Kogushi, Ube, Yamaguchi 755-8505, Japan, umemoto@yamaguchi-u.ac.jp.

Conflicts of Interest

The remaining authors declare no conflicts of interest.

treatment reversed these changes compared to that seen in the mice treated with AngII alone. NE produced little effect on any of the indices in either the WT or T1r4$^{lps\text{-}d}$ mice.

Conclusions—TLR4 may be involved in the processes underlying the increased oxidative stress, selectively activated MCP-1 expression and cardiac hypertrophy and dysfunction seen in cases of AngII-induced hypertension.

Keywords

Hypertension; Cardiac hypertrophy; Toll-like receptor 4; Monocyte chemoattractant protein-1; Angiotensin II; Mouse

Introduction

The activation of the renin-angiotensin system plays an important role in the pathogenesis of hypertension. Specifically, the direct cardiac effects of angiotensin II (AngII) contribute to the pathogenesis and progression of cardiac hypertrophy and fibrosis via the production of oxidative stress and inflammation[1,2], both systolic and diastolic dysfunction[3,4] characterized by the signs and symptoms of heart failure and a preserved ejection fraction and abnormal left ventricular (LV) diastolic function caused by decreased LV compliance and relaxation[5]. Cardiac hypertrophy may be reversed by the administration of angiotensin II type 1 (AT1) receptor antagonists[6].

The Toll-like receptor (TLR) family is a major component of pathogen-associated molecular pattern-recognition molecules[7], and the heart has been suggested to possess an innate immune system[8]. For example, TLR4 knockout mice develop less-severe LV hypertrophy following aortic banding compared to matched wild-type animals[9]. Another study revealed that an enhanced TLR4 expression may be linked to the development and maintenance of hypertension[10]. TLRs are also activated by endogenous signals, such as oxidative stress and heat shock proteins, and are expressed by cardiomyocytes[11]. TLR4 activation is also reported to be an important mediator of maladaptive LV remodeling and dysfunction as well as a reduced survival after myocardial infarction[12]. Moreover, it has been demonstrated that TLR4 polymorphism is associated with LV hypertrophy and the inflammatory response in humans[13, 14], suggesting that TLR4 is involved in the development of LV hypertrophy.

Both AngII and TLR4 activate NADPH oxidase to produce reactive oxygen species (ROS), followed by the activation of proinflammatory transcription factors, such as nuclear factor-κB (NF-κB); these factors stimulate the expression of monocyte chemoattractant protein-1 (MCP-1) and may play a role in the development of hypertension[15–17]. However, it remains unknown whether TLR4 modulates AngII signal transduction[18] or is involved in the proinflammatory process activated by AngII[19]. In order to clarify whether TLR4 is involved in the cardiac hypertrophy and dysfunction induced by AngII stimulation, we investigated the effects of TLR4 on oxidative stress, inflammation and the cardiac function and hypertrophy in mice with AngII-induced hypertension.

Methods

The Ethics Committee for Animal Experimentation at the Yamaguchi University School of Medicine approved the experimental protocol used in this study.

Chemicals and Antibodies

AngII acetate hydrate and L-(−)-norepinephrine bitartrate salt monohydrate were purchased from Sigma-Aldrich (St. Louis, MO). Irbesartan (IRB), a selective ATI receptor antagonist, was kindly provided by Shionogi Pharmaceutical (Tokyo). The immunohistochemical and immunoblot analyses used rabbit polyclonal antibodies against human phospho (p)-NF-κB p65 (ser 536) and MCP-1 (Cell Signaling Technology, Beverly, MA) and rat monoclonal antibodies against the monocyte/macrophage marker MOMA-2 (BMA Biomedicals, August, Switzerland).

Animals and Experimental Protocols

Male 12- to 16-week-old wild-type (WT) mice (BALB/c, $n = 24$; Charles River Japan, Yokohama, Japan) and homozygous BALB/c background mice (C.C3H–Tlr4$^{lps\text{-}d}$, Jackson Laboratory, Bar Harbor, ME, Tlr4$^{lps\text{-}d}$ mice; $n = 24$)[11,20,21] were maintained at the Science Research Center of Yamaguchi University.

WT and T1r4$^{lps\text{-}d}$ mice were randomized into four groups each and treated with physiological saline (control group; $n = 6$), AngII (1.1 mg·kg^{-1}· day^{-1}, AngII-treated group; $n = 6$), norepinephrine (5.6 mg ·kg^{-1} · day^{-1}, NE-treated group; $n = 6$) or a subdepressor dose of IRB with AngII (IRB 6 mg · kg^{-1}· · day^{-1}, IRB-treated group; $n = 6$). The doses used in the experiments were determined in preliminary experiments.

Anesthesia was induced in the mice using isoflurane (Abbott Japan, Tokyo) at a concentration of 3% and subsequently maintained at 1% via a face mask during the implantation of osmotic minipumps (Model 1002; ALZET Osmotic Pumps, Cupertino, CA) and transthoracic echocardiography.

Physiological saline, AngII and NE were administered subcutaneously using osmotic minipumps for two weeks. IRB was given in drinking water in association with the AngII treatment for two weeks. The heart and body weights were evaluated after the two-week treatment period, and the systolic blood pressure and heart rate were measured using tail-cuff plethysmography without anesthesia on the seventh and 14th days during the experiment.

In Vivo Transthoracic Cardiac Imaging

Three mice from each group were subjected to transthoracic echocardiography using an HDI-5000 ultrasound machine (Philips, Amsterdam, Netherlands) equipped with a 15-MHz probe. The mice were examined in the supine position with closed chests, and the transducer was gently placed in the left parasternal position. An M-mode echocardiogram of the left ventricle was obtained to measure the chamber diameters and end-diastolic and end-systolic thicknesses of the interventricular septum and posterior wall. LV fractional shortening

(%FS) was calculated as follows: 100 × [LV end-diastolic dimension (LVEDd) – LV end-systolic dimension (LVESd)]/LVEDd (%).

In addition, the peak velocities of the early ventricular filling wave (E wave) and late ventricular filling wave caused by atrial contraction (A wave) of the transmitral flow were measured using mitral Doppler flow spectra, and the E/A ratio was calculated as an index to estimate the LV diastolic function. Standard basic echocardiography measurements and calculations were performed as previously described[22,23] Representative echocardiogram images are shown in Fig. 1A.

Tissue Preparation

After the completion of the two-week treatment period, the mice were euthanized under inhalation anesthesia with an excessive dose of isoflurane. The left ventricles of the hearts were subsequently separated, washed with heparinized saline, weighed and cut into four pieces perpendicular to the long axis. A piece of the middle portion of the heart tissue from each heart was snap frozen with optimal cutting temperature (OCT) compound in liquid nitrogen to obtain fresh frozen, 40-μm-thick sections for dihydroethidium (DHE) staining[24,25]. The other middle portion of the heart, which was fixed in 10% buffered formaldehyde, was embedded in paraffin and sectioned into 4-μm slices for assessments of the expression levels of pNF-κB and MCP-1 and morphology using Masson Trichrome or hematoxylin-eosin (HE) staining. The rest of the base and apex-side heart tissues were frozen in liquid nitrogen and stored at −80 °C until use in the other experiments[25].

Histological and Immunohistochemical Analyses

The sections were quantified morphometrically using a camera control program system (ACT-1, version 2.51) with a digital camera (DXM1200F; Nikon, Tokyo) connected to an automated microscope (Eclipse El000, Nikon). The wall-to-lumen ratio and degree of perivascular fibrosis of the intramyocardial artery were assessed using Masson Trichrome staining, as previously reported[26, 27] Immunohistochemistry was also performed to determine the expression levels of pNF-κB, MCP-1 and the monocyte/macrophage marker MOMA-2 in the heart tissues according to the avidin-biotinylated enzyme complex method (Vector Laboratories, San Francisco, CA) [27] The parameters for pNF-κB and MCP-1 were evaluated using a computer-assisted image analysis system with the NIH Image 1.62 software program, as previously reported[28]. The total number of MOMA-2-positive cells in the mouse heart was counted in eight randomly selected high-power fields per tissue section for 3–6 mice in each group. The mean values for each heart were used for the statistical analysis.

In Situ Evaluation of $\cdot O_{2-}$ in the Heart

Unfixed frozen heart tissues in 30-μm-thick segments were prepared for *in situ* imaging of ROS generation in the myocardium. The $\cdot O_{2-}$ content was evaluated using fluorescent DHE 2 μmol/L (Polysciences, Warrington, PA), as previously described[25, 27]. The specificity of DHE signals for $\cdot O_{2-}$ detection was confirmed via preincubation with superoxide dismutase (SOD)-mimetic Tempol (500 U/mL), and the images were obtained with a laser scanning

confocal microscope (LSM510; Zeiss, Munich, Germany). The data are expressed as the percentage of the corresponding data for the control WT mice.

NADPH Oxidase Activity in the Heart

The NADPH oxidase activity was determined using a luminescence assay[25]. Briefly, the heart tissues were placed in a chilled, modified Krebs-hydroxyethyl piperazineethanesulfonic acid (HEPES) buffer (99 mmol/L NaCl, 4.7 mmol/L KC1, 1.9 mmol/L $CaC1_2$, 1.2 mmol/L $MgSO_4$, 1.0 mmol/L K_2HPO_4, 25 mmol/L NaHCO3, 20 mmol/L Na-HEPES and 11 mmol/L glucose, pH 7.4), after which a 10% (w/v) tissue homogenate in 50 mmol/L of phosphate buffer was subjected to centrifugation at 1,000 ×*g* for 10 minutes to remove unbroken cells and debris. An aliquot was kept for protein determination, and the supernatants (25 μL) were assayed immediately for superoxide production. A luminescence assay was performed in 50 mmol/L of phosphate buffer, pH 7.0, containing 1 mmol/L of EGTA, 150 mmol/L of sucrose, 5 μmol/L of lucigenin (bis-N-methylacridinium nitrate) as the electron acceptor and 100 μmol/L of NADPH as the substrate (final volume, 225 μL), all of which was poured into a 96-well microplate.

This concentration fell well within the linear range of the assay (1 μmol/L to 10 mmol/L for NADPH), and NADPH was not rate-limiting over the initial course of the test. No activity was detected in the absence of NADPH. Following dark adaptation, the background counts were recorded, and the tissue homogenate was added to the microplate. The lucigenin count was recorded every 10 seconds for 10 minutes, and the respective background counts (without tissue homogenate) were subtracted from the tissue homogenate readings. The lucigenin count is expressed as the count per minute per microgram of tissue homogenate.

Protein Isolation and Immunoblot Analyses

Proteins were extracted from the frozen heart tissues homogenized in 25 mM Tris (pH 7.4), containing 150 mM NaCl, 5 mM ethylenediaminetetraacetic acid, 10 mM sodium pyrophosphate, 10 mM β-glycerophosphate, 1 mM Na_3VO_4, 1 mM phenylmethane sulfonyl fluoride and 10 mg/mL of aprotinin, with Triton X-100 added to a final concentration of 1%, in order to extract the proteins. The protein concentrations were determined using a BCA protein assay kit (Bio-Rad, Hercules, CA).

Immunoblotting was performed as previously described[29]. Briefly, equal amounts of sample proteins were loaded in each lane of a sodium dodecyl sulfate polyacrylamide gel, transferred onto polyvinylidene difluoride membranes (Millipore, Bedford, MA) and probed with mouse monoclonal antibodies against pNF-κB p65 (ser 536, Cell Signaling Technology, #3036) and glyceraldehyde 3-phosphate dehydrogenase (GAPDH, Millipore; #MAB374). The target proteins, pNF-κB and GAPDH, were visualized with the use of a chemiluminescence detection kit (Thermo Scientific, Rockford, IL). The protein levels of MCP-1 in the heart tissues were quantified according to the sandwich enzyme immunoassay technique using the Mouse CCL2/JE/MCP-1 Quantikine ELISA Kit (Catalog No. MJE00, R&D Systems, Minneapolis, MN), based on the manufacturer's instructions.

Statistical Analysis

All values are expressed as the mean ±SE. The experimental groups were compared using an analysis of variance (ANOVA) followed by Scheffe's multiple comparison method. *P*-values of < 0.05 were accepted as being significant.

Results

Body Weight, Blood Pressure, Left Ventricular Weight, Left Ventricular Weight/Body Weight, Wall-to-lumen Ratio and Perivascular Fibrosis in the Intramyocardial Artery

Throughout the present experiments, the control WT and T1r4$^{lps\text{-}d}$ mice showed similar body weights and heart rates, and the drug treatment did not affect these indices. As shown in Table 1, AngII and NE similarly and significantly increased systolic blood pressure in all drug-treated groups compared to that observed in the control WT and T1r4$^{lps\text{-}d}$ mice. Few differences in blood pressure were observed among the drug-treated groups. In the WT mice, Angll significantly increased the LV weight/body weight ratio, whereas little effect was seen in the T1r4$^{lps\text{-}d}$ mice. In the WT mice, the IRB treatment significantly rescued the increase in LV weight/body compared to that observed in the mice receiving AngII-treatment alone (Table 1).

AngII also significantly increased both the wall-to-lumen ratio and degree of perivascular fibrosis of the intramyocardial arteries in the WT mice, whereas the T1r4$^{lps\text{-}d}$ mice showed little changes following AngII treatment with respect to this index. In the WT mice, IRB treatment significantly rescued the increase in the wall-to-lumen ratio compared to that noted in the mice that received AngII treatment alone (Table 1). The extent of perivascular fibrosis of the intramyocardial arteries did not differ between the AngII + IRB group and the AngII treatment group in the WT mice. Although the degree of perivascular fibrosis of the intramyocardial arteries in the AngII + IRB group was slightly lower than that observed in the AngII-treated WT mice and higher than that seen in the other groups, the differences were not significant (Table 1 and Fig. 1B).

TLR4 Deficiency Inhibited the AngII-Induced Cardiac Hypertrophy and Dysfunction Assessed on Echocardiography

In the WT mice, AngII induced a significant increase in the LV wall thickness and LVESd values and a significant decrease in the %FS and E/A ratio of the transmitral flow. In contrast, the T1r4$^{lps\text{-}d}$ mice showed little effects following AngII administration with respect to these indices. The LVEDd values were not affected by any drug treatment, and NE did not produce any significant effects on these indices in either the WT or Tlr4$^{lps\text{-}d}$ mice. In the WT mice, IRB treatment significantly rescued the increase in LV wall thickness and caused a significant decrease in the %FS and E/A ratio of the transmural flow compared to that noted in the mice in the AngII-treatment alone group (Table 2).

TLR4 Deficiency Abolished the AngII-Induced ROS in the Heart

Fig. 2A provides representative figures of DHE staining used to assess the $\cdot O_{2-}$ content in the mouse heart. The control WT and Tlr4$^{lps\text{-}d}$ mice showed minimal fluorescence in the heart. In the quantitative analysis, the AngII-treated WT mice exhibited five-fold higher

values for DHE fluorescence than the control WT mice, reflecting increased $\cdot O_{2-}$ content in the heart, and IRB significantly reduced the DHE density compared with that seen in the AngII-treatment alone group (Fig.2B).

In the presence of the SOD mimetic Tempol, DHE fluorescence was markedly decreased in the heart, suggesting that DHE staining primarily reflects an increase in $\cdot O_{2-}$ in the heart (Fig.2A). In contrast, the DHE density in the AngII-treated T1r4$^{lps\text{-}d}$ mice was markedly suppressed compared to that observed in the AngII-treated WT mice and was not affected by IRB treatment. NE slightly increased the DHE density in both the WT and T1r4$^{lps\text{-}d}$ mice, although this increase did not reach the level of significance (Fig. 2B).

TLR4 Deficiency Inhibited the AngII-Induced NADPH Oxidase Activity in the Heart

We assessed the NADPH oxidase activity in the heart using a luminescence assay (Fig. 2C). AngII significantly increased the myocardial NADPH oxidase activity by five-fold, only in the WT mice, and treatment with a subdepressor dose of IRB prevented this increase. Among the NE-treated groups, the WT and T1r4$^{lps\text{-}d}$ mice showed a slight increase in the NADPH oxidase activity in the heart, with little difference from that seen in the control WT and T1r4$^{lps\text{-}d}$ mice (Fig. 2C).

TLR4 Deficiency Abolished the AngII-Induced Infiltration of Monocytes/Macrophages and Upregulation of MCP-1, but Not pNF-κB, in the Heart

Immunohistochemically, monocytes/macrophages stained brown in the interstitial tissue of the mouse heart (Fig.3A). In the WT mice, the degree of infiltration of monocytes/macrophages in the heart remarkably increased following AngII treatment compared to that observed in the control WT mice, and this change was suppressed with IRB treatment. In contrast, infiltration of monocytes/macrophages in the heart was scarcely observed in the control T1r4$^{lps\text{-}d}$ mice and remained unaffected by AngII or IRB treatment. Meanwhile, NE treatment did not affect the increase in the infiltration of monocytes/macrophages in the heart compared to that noted in the controls among both the WT and T1r4$^{lps\text{-}d}$ mice. A quantitative analysis demonstrated that the infiltration of monocytes/macrophages in the hearts increased by 20-fold following AngII treatment compared to that seen in the controls among the WT mice, and this infiltration was suppressed with IRB treatment. In contrast, infiltration of monocytes/macrophages in the hearts in the T1r4$^{lps\text{-}d}$ mice remained unaffected by AngII or IRB treatment (Fig.3B), whereas NE treatment had little effect on the infiltration of monocytes/macrophages in the hearts compared to that observed in the controls among both the WT and T1r4$^{lps\text{-}d}$ mice (Fig. 3B).

pNF-κB stained brown in the cytoplasm and nuclei of the myocardial cells, whereas MCP-1 stained brown only in the cytoplasm (Fig.3A). The quantitative analysis showed similar levels of expression in the heart in the control WT and T1r4$^{lps\text{-}d}$ mice for both pNF-κB and MCP-1 (Fig.3C, D). In the WT and T1r4$^{lps\text{-}d}$ mice, AngII increased the expression of pNF-κB in the heart by two-fold compared to that noted in the control WT and T1r4$^{lps\text{-}d}$ mice, although IRB treatment inhibited this increase (Fig.3C). In the WT mice, the expression of MCP-1 in the heart was increased 2.5-fold by AngII treatment compared to that seen in the controls, and this expression was suppressed with IRB treatment, whereas the MCP-1

expression in the heart in the T1r4$^{lps\text{-}d}$ mice remained unaffected by AngII or IRB (Fig. 3D). NE treatment resulted in little increase in the expression levels of pNF-κB or MCP-1 in the heart compared to that seen in the controls among both the WT and T1r4$^{lps\text{-}d}$ mice (Fig. 3C, D).

Discussion

The present results demonstrate that TLR4 plays an important role in the onset of cardiac hypertrophy and functional impairment in the setting of AngII-induced hypertension. It has been reported that the cardiac renin-angiotensin system is activated by pressure overload and/or heart failure[30] and that cardiac local AngII formation in the myocardium appears to be regulated independently from the circulating renin-angiotensin system and is abolished by the administration of AT1 receptor antagonist[30]. Meanwhile, TLR4 plays a pivotal role within the innate immune system and contributes to the host defense against exogenous microbial pathogens by detecting exogenous ligands[7]. TLR4 has also been shown to be stimulated by endogenous ligands under conditions of inflammation and oxidative stress[11,31,32].

Using aortic banding techniques, Ha *et al.* demonstrated that the absence of TLR4 abolishes the increase in cardiac mass and myocyte size and reduces the NF-κB expression and resultant pressure overload[9], suggesting that TLR4 is a relevant receptor in heart muscle that mediates cardiac hypertrophy *in vivo*. Timmers *et al.* also reported that knockdown of TLR4 reduces the extent of LV remodeling and preserves the systolic function without affecting the infarct size after myocardial infarction[11], indicating that TLR4 plays a causal role in post-infarct maladaptive ventricular remodeling. The present experimental model also demonstrated that AngII induces cardiac hypertrophy and depresses the systolic and diastolic functions, as in the pressure overload model[3,5], and that TLR4 deficiency inhibits AngII-induced cardiac hypertrophy and dysfunction, independent of the blood pressure level, indicating that TLR4 may be involved downstream of the AngII signaling pathway.

A recent study employing a specific chemical TLR4 blocker revealed that AngII-induced hypertensive effects are mediated, in part, by brain TLR4 and that the intracerebroventricular administration of brain TLR4 blockade attenuates the AngII-induced hypertensive response, possibly via the downregulation of myocardial inflammatory molecules and sympathetic activity in rats[33]. In contrast, the T1r4$^{lps\text{-}d}$ mice used in the current study are a congenic mutant strain, and it is thus unknown whether TLR4 present in the brain is similarly involved in the onset of AngII-induced hypertension.

We also observed that cardiac fibrosis was not decreased by IRB treatment in the AngII-treated WT mice, as shown in Table 1. It has been reported that cardiac fibrosis is important for the adaptation of the murine heart to pressure overload; cardiac fibroblasts are absolutely required for protection of the cardiac function under conditions of severe pressure overload in order to maintain the cardiac structure against high blood pressure and play essential roles in both cardio-protection and cardiomyocyte hypertrophy. Hence, cardiac myocytes are not mere bystanders acting only in the process of fibrosis, but are also crucial mediators of myocardial hypertrophy and adaptive responses in the heart[34]. This previous report

potentially supports the results of the present study regarding the degree of cardiac fibrosis and effects of AngII + IRB treatment in WT mice, since the blood pressure did not change in these mice compared to that seen in the WT mice treated with AngII alone. The role of TLR4 in this cardiac fibrosis response warrants further investigation.

Hypertension induces remodeling, leading to functional consequences associated with heart failure[3, 4], which involves excess parallel signal transduction events[35,36]. Innate immunity is activated in the injured heart in different ways and is evident in the form of cytokine release from the heart and the activation of TLRs that play a role in recognizing danger as well as NF-κB, which regulates gene programs involved in inflammation[8, 11,37]. It has also been reported that the renin-angiotensin system is crucial for NADPH oxidase-dependent redox signaling pathways, which provoke the upregulation of MCP-1; this process has been shown to be blunted by an AT1 receptor antagonist[38]. The results of the present study indicate that the activation of NF-κB may be caused solely by AngII, since the increase in NF-κB was induced without an increase in ROS and inhibited by the administration of a subdepressor dose of an AT1 receptor antagonist. In addition, MCP-1 was not increased in the TLR4-deficient mice, indicating that TLR4 may also be involved in this process after the activation of NF-κB and prior to the upregulation of MCP-1[39]. This suggests that the TLR4 function may be essential for the upregulation of NADPH oxidase-dependent ROS signaling and the inflammatory process, followed by the onset of cardiac hypertrophy and cardiac dysfunction induced by AngII administration.

However, it has also been reported that NF-κB activation upregulates NADPH oxidase activation[40]. Therefore, although it is possible that TLR4 is involved in the NF-κB-induced amplification of NADPH oxidase activation, it is unlikely that TLR4 signaling mediates the first phase of NADPH oxidase activation that occurs soon after AT1 activation. In addition, we cannot exclude the possibility that TLR4 regulates NF-κB signaling (as in the case of NF-κ B-DNA binding), or that it independently regulates cardiac hypertrophy and fibrosis and/or the MCP-1 expression by other mechanisms, such as the peroxisome proliferator-activated receptor-γ coactivator-1 axis in the murine heart[41].

Furthermore, it was recently reported that AngII infusion induces cardiac injury (including increased monocyte adherence to endothelia cells and macrophage infiltration, the expression of inflammatory cytokines and cardiac fibrosis), whereas inhibiting the effects of AngII inhibited these changes in a mouse model heart[42]. In the present study, we also showed similar effects of AngII on monocyte and macrophage infiltration in the hearts in the WT mice, but not TLR4-deficient mice, suggesting that the TLR4 signaling pathway is essential for these inflammatory processes and may be an important determining factor for the LV function via the effects of oxidative stress-induced inflammation, such as that associated with MCP-1.

We did not evaluate hormonal indices of cardiac dysfunction, such as the levels of N-terminal pro-brain natriuretic peptide. However, the indices evaluated on echocardiography in this study are correlated with the cardiac function in patients with hypertension[43]. The impact of the activation of innate cardiac immunity on the long-term outcomes in *in vivo* models of hypertrophy and remodeling remains unclear, with conflicting results as to

whether it is beneficial or detrimental[11]. Further research using different models that evoke cardiac remodeling is therefore required, as is long-term follow-up, to determine whether activation of the innate immune system, including TLR4, is beneficial or detrimental in models of chronic hypertensive cardiac remodeling[37].

Finally, we did not examine the effects of AngII on the expression levels of the AngII receptor, Ang-converting enzyme or chemokine receptors in the hearts in the TLR4-deficient mice. It has been reported that that the central blockade of TLR4 in AngII-infused rats delays the progression of hypertension, reduces cardiac hypertrophy and dysfunction, attenuates the expression of the myocardial pro-inflammatory cytokines, gp91phox, a component of NADPH oxidase, and NF-κB and inhibits angiotensin-converting enzyme and AngII type 1 receptors in the heart[33]. Moreover, it has been reported that TLR4 agonists downregulate two major chemokine receptors on monocytic cells[44]. Taken together with the present findings, these observations suggest that the AngII receptor signaling pathway may be involved in the pathogenesis of cardiac hypertrophy and dysfunction and that the blood pressure level may be dependent on the AngII receptor signaling pathway, as TLR4 may be necessary to produce oxidative stress in the heart induced by AngII stimulation. Further research is thus needed to confirm the expression levels of these parameters in the mouse heart.

In conclusion, we herein demonstrated that TLR4 may be involved in the increase in oxidative stress, as well as selectively activating MCP-1 and inducing the onset of cardiac hypertrophy and dysfunction, in the setting of AngII-induced hypertension. These data provide the first evidence of a causal role of TLR4 in the development of AngII-induced cardiac hypertrophy and dysfunction. TLR4 inhibition may therefore constitute a novel therapeutic approach to inhibiting the mechanisms underlying hypertensive cardiac hypertrophy and dysfunction in patients with hypertension.

Acknowledgments

Acknowledgements and Notice of Grant Support

We thank Dr. Hiroko Yoshino for her critical role in this study and Ms. Ishihara, Ms. Okamoto and Ms. Oishi for their excellent technical assistance. This work was supported in part by JSPS KAKENHI Grant Nos. 18590776, 21590954 and 24591115 to S.U., the 11th New Frontier Project of Yamaguchi University Graduate School of Medicine and Yamaguchi University Hospital to S.U., and the first and third Research Meetings on Kidney Disease and Hypertension to S.U., and NIH R01 HL070187 to T.F, respectively.

Irbesartan, a selective AT1 receptor antagonist, was kindly provided by Shionogi Pharmaceutical (Tokyo, Japan). S.U. received a consultant fee from Boehringer Ingelheim Japan Inc., honoraria from Kyowa Hakko Kirin Co., Ltd., Takeda Pharmaceutical Co., Ltd., Mochida Pharmaceutical Co., Ltd., Eisai Co., Ltd. and Asuka Pharmaceutical Co., Ltd. and a grant from Maruha Nichiro Holdings, Inc.

References

1. Kurdi M, Booz GW. New take on the role of angiotensin II in cardiac hypertrophy and fibrosis. Hypertension. 2011; 57:1034–1038. [PubMed: 21502563]
2. Touyz RM, Briones AM. Reactive oxygen species vascular biology: implications in human hypertension. Hypertens Res. 2011; 34:5–14. [PubMed: 20981034]
3. Chinnaiyan KM, Alexander D, McCullough PA. Role of angiotensin II in the evolution of diastolic heart failure. J Clin Hypertens (Greenwich). 2005; 7:740–747. [PubMed: 16330897]

4. Kono M, Kisanuki A, Ueya N, Kubota K, Kuwahara E, Takasaki K, Yuasa T, Mizukami N, Miyata M, Tei C. Left ventricular global systolic dysfunction has a significant role in the development of diastolic heart failure in patients with systemic hypertension. Hypertens Res. 2010; 33:1167–1173. [PubMed: 20720552]
5. Lalande S, Johnson BD. Diastolic dysfunction: a link between hypertension and heart failure. Drugs Today (Barc). 2008; 44:503–513. [PubMed: 18806901]
6. Li L, Zhou N, Gong H, Wu J, Lin L, Komuro I, Ge J, Zou Y. Comparison of angiotensin II type 1-receptor blockers to regress pressure overload-induced cardiac hypertrophy in mice. Hypertens Res. 2010; 33:1289–1297. [PubMed: 20944638]
7. Kumar H, Kawai T, Akira S. Pathogen recognition by the innate immune system. Int Rev Immunol. 2011; 30:16–34. [PubMed: 21235323]
8. Mann DL. The emerging role of innate immunity in the heart vascular system: for whom the cell tolls. Circ Res. 2011; 108:1133–1145. [PubMed: 21527743]
9. Ha T, Li Y, Hua F, Ma J, Gao X, Kelley J, Zhao A, Had-dad GE, Williams DL, William Browder I, Kao RL, Li C. Reduced cardiac hypertrophy in toll-like receptor 4-deficient mice following pressure overload. Cardiovasc Res. 2005; 68:224–234. [PubMed: 15967420]
10. Eissler R, Schmaderer C, Rusai K, Kuhne L, Sollinger D, Lahmer T, Witzke O, Lutz J, Heemann U, Baumann M. Hypertension augments cardiac Toll-like receptor 4 expression and activity. Hypertens Res. 2011; 34:551–558. [PubMed: 21248757]
11. Timmers L, Sluijter JR, van Keulen JK, Hoefer IE, Neder-hoff MG, Goumans MJ, Doevendans PA, van Echteld CJ, Joles JA, Quax PH, Piek JJ, Pasterkamp G, de Kleijn DP. Toll-like receptor 4 mediates maladaptive left ventricular remodeling and impairs cardiac function after myocardial infarction. Circ Res. 2008; 102:257–264. [PubMed: 18007026]
12. Landmesser U, Wollert KC, Drexler H. Potential novel pharmacological therapies for myocardial remodelling. Cardiovasc Res. 2009; 81:519–527. [PubMed: 19019834]
13. Sales ML, Schreiber R, Ferreira-Sae MC, Fernandes MN, Piveta C, Cipolli JA, Calixto A, Matos-Souza JR, Geloneze B, Franchini KG, Nadruz W Jr. The functional Toll-like receptor 4 Asp299Gly polymorphism is associated with lower left ventricular mass in hypertensive women. Clin Chim Acta. 2010; 411:744–748. [PubMed: 20146922]
14. Sales ML, Schreiber R, Ferreira-Sae MC, Fernandes MN, Piveta CS, Cipolli JA, Cardoso CC, Matos-Souza JR, Geloneze B, Franchini KG, Nadruz W Jr. Toll-like receptor 6 Ser249Pro polymorphism is associated with lower left ventricular wall thickness and inflammatory response in hypertensive women. Am J Hypertens. 2010; 23:649–654. [PubMed: 20224557]
15. Harrison DG, Guzik TJ, Lob HE, Madhur MS, Marvar PJ, Thabet SR, Vinh A, Weyand CM. Inflammation, immunity, and hypertension. Hypertension. 2011; 57:132–140. [PubMed: 21149826]
16. Eißler R, Schmaderer C, Rusai K, Kühne L, Sollinger D, Lahmer T, Witzke O, Lutz J, Heemann U, Baumann M. Hypertension augments cardiac Toll-like receptor 4 expression and activity. Hypertens Res. 2011; 34:551–555. [PubMed: 21248757]
17. Iwai M, Mogi M, Horiuchi M. Role of NAD(P)H oxidase and its regulation in chronic hypertension. Hypertens Res. 2006; 29:743–744. [PubMed: 17283859]
18. Lemarie CA, Schiffrin EL. The angiotensin II type 2 receptor in cardiovascular disease. J Renin Angiotensin Aldosterone Syst. 2010; 11:19–31. [PubMed: 19861349]
19. Brasier AR. The nuclear factor-kappaB-interleukin-6 signalling pathway mediating vascular inflammation. Cardiovasc Res. 2010; 86:211–218. [PubMed: 20202975]
20. Vogel SN, Wax JS, Perera PY, Padlan C, Potter M, Mock BA. Construction of a BALB/c congenic mouse, C.C3H-Lpsd, that expresses the Lpsd allele: analysis of chromosome 4 markers surrounding the Lps gene. Infect Immun. 1994; 62:4454–4459. [PubMed: 7927709]
21. Poltorak A, He X, Smirnova I, Liu M-Y, Huffel CV, Du X, Birdwell D, Alejos E, Silva M, Galanos C, Freudenberg M, Ricciardi-Castagnoli P, Layton B, Beutler B. Defective LPS Signaling in C3H/HeJ, C57BL/10ScCr Mice: Mutations inTlr4 Gene. Science. 1998; 282:2085–2088. [PubMed: 9851930]

22. Zhou YQ, Zhu Y, Bishop J, Davidson L, Henkelman RM, Bruneau BG, Foster FS. Abnormal cardiac inflow patterns during postnatal development in a mouse model of Holt-Oram syndrome. Am J Physiol Heart Circ Physiol. 2005; 289:H992–H1001. [PubMed: 15849237]
23. Yamada M, Ikeda Y, Yano M, Yoshimura K, Nishino S, Aoyama H, Wang L, Aoki H, Matsuzaki M. Inhibition of protein phosphatase 1 by inhibitor-2 gene delivery ameliorates heart failure progression in genetic cardiomyopathy. FASEB J. 2006; 20:1197–1199. [PubMed: 16627625]
24. Umeji K, Umemoto S, Itoh S, Tanaka M, Kawahara S, Fukai T, Matsuzaki M. Comparative effects of pitavastatin and probucol on oxidative stress, Cu/Zn superoxide dismutase, PPAR-gamma, and aortic stiffness in hypercholesterolemia. Am J Physiol Heart Circ Physiol. 2006; 291:H2522–2532. [PubMed: 16844911]
25. Hashimoto R, Umemoto S, Guo F, Umeji K, Itoh S, Kishi H, Kobayashi S, Matsuzaki M. Nifedipine activates PPARgamma and exerts antioxidative action through Cu/ ZnSOD independent of blood-pressure lowering in SHRSP. J Atheroscler Thromb. 2010; 17:785–795. [PubMed: 20460829]
26. Kawahara S, Umemoto S, Tanaka M, Umeji K, Matsuda S, Kubo M, Matsuzaki M. Up-regulation of Akt and eNOS induces vascular smooth muscle cell differentiation in hypertension in vivo. J Cardiovasc Pharmacol. 2005; 45:367–374. [PubMed: 15772527]
27. Itoh S, Umemoto S, Hiromoto M, Toma Y, Tomochika Y, Aoyagi S, Tanaka M, Fujii T, Matsuzaki M. Importance of NAD(P)H oxidase-mediated oxidative stress and contractile type smooth muscle myosin heavy chain SM2 at the early stage of atherosclerosis. Circulation. 2002; 105:2288–2295. [PubMed: 12010912]
28. Kubo M, Umemoto S, Fujii K, Itoh S, Tanaka M, Kawahara S, Matsuzaki M. Effects of angiotensin II type 1 receptor antagonist on smooth muscle cell phenotype in intramyocardial arteries from spontaneously hypertensive rats. Hypertens Res. 2004; 27:685–693. [PubMed: 15750263]
29. Yoshimura K, Aoki H, Ikeda Y, Fujii K, Akiyama N, Furutani A, Hoshii Y, Tanaka N, Ricci R, Ishihara T, Esato K, Hamano K, Matsuzaki M. Regression of abdominal aortic aneurysm by inhibition of c-Jun N-terminal kinase. Nat Med. 2005; 11:1330–1338. [PubMed: 16311603]
30. Wollert KC, Drexler H. The renin-angiotensin system and experimental heart failure. Cardiovasc Res. 1999; 43:838–849. [PubMed: 10615411]
31. Ohashi K, Burkart V, Flohe S, Kolb H. Cutting edge: heat shock protein 60 is a putative endogenous ligand of the toll-like receptor-4 complex. J Immunol. 2000; 164:558–561. [PubMed: 10623794]
32. Okamura Y, Watari M, Jerud ES, Young DW, Ishizaka ST, Rose J, Chow JC, Strauss JF 3rd. The extra domain A of fibronectin activates Toll-like receptor 4. J Biol Chem. 2001; 276:10229–10233. [PubMed: 11150311]
33. Dange RB, Agarwal D, Masson GS, Vila J, Wilson B, Nair A, Francis J. Central blockade of TLR4 improves cardiac function and attenuates myocardial inflammation in angiotensin II-induced hypertension. Cardiovasc Res. 2014; 103:17–27. [PubMed: 24667851]
34. Takeda N, Manabe I, Uchino Y, Eguchi K, Matsumoto S, Nishimura S, Shindo T, Sano M, Otsu K, Snider P, Conway SJ, Nagai R. Cardiac fibroblasts are essential for the adaptive response of the murine heart to pressure overload. J Clin Invest. 2010; 120:254–265. [PubMed: 20038803]
35. Paravicini TM, Touyz RM. Redox signaling in hypertension. Cardiovasc Res. 2006; 71:247–258. [PubMed: 16765337]
36. Vogel V, Bokemeyer D, Heller J, Kramer HJ. Cardiac hypertrophy in the Prague-hypertensive rat is associated with enhanced JNK2 but not ERK tissue activity. Kidney Blood Press Res. 2001; 24:52–56. [PubMed: 11174007]
37. Valen G. Innate immunity and remodelling. Heart Fail Rev. 2011; 16:71–78. [PubMed: 20694832]
38. Kamioka M, Ishibashi T, Sugimoto K, Uekita H, Nagai R, Sakamoto N, Ando K, Ohkawara H, Teramoto T, Maruyama Y, Takeishi Y. Blockade of renin-angiotensin system attenuates advanced glycation end products-mediated signaling pathways. J Atheroscler Thromb. 2010; 17:590–600. [PubMed: 20379053]
39. Yang J, Jiang H, Ding JW, Chen LH, Li S, Zhang XD. Valsartan preconditioning protects against myocardial ischemia-reperfusion injury through TLR4/NF-kappaB signaling pathway. Mol Cell Biochem. 2009; 330:39–46. [PubMed: 19370315]

40. Anrather J, Racchumi G, Iadecola C. NF-kappaB regulates phagocytic NADPH oxidase by inducing the expression of gp91phox. J Biol Chem. 2006; 281:5657–5667. [PubMed: 16407283]

41. Schilling J, Lai L, Sambandam N, Dey CE, Leone TC, Kelly DP. Toll-like receptor-mediated inflammatory signaling reprograms cardiac energy metabolism by repressing peroxisome proliferator-activated receptor gamma coactivator-1 signaling. Circ Heart Fail. 2011; 4:474–482. [PubMed: 21558447]

42. Wang Y, Li Y, Wu Y, Jia L, Wang J, Xie B, Hui M, Du J. 5TNF-alpha and IL-lbeta neutralization ameliorates angiotensin II-induced cardiac damage in male mice. Endocrinology. 2014; 155:2677–2687. [PubMed: 24877626]

43. Ceyhan C, Unal S, Yenisey C, Tekten T, Ceyhan FB. The role of N terminal pro-brain natriuretic peptide in the evaluation of left ventricular diastolic dysfunction: correlation with echocardiographic indexes in hypertensive patients. Int J Cardiovasc Imaging. 2008; 24:253–259. [PubMed: 17687631]

44. Parker LC, Whyte MKB, Vogel SN, Dower SK, Sabroe I. Toll-like receptor (TLR)2 and TLR4 agonists regulate CCR expression in human monocytic cells. J Immunol. 2004; 172:4977–4986. [PubMed: 15067079]

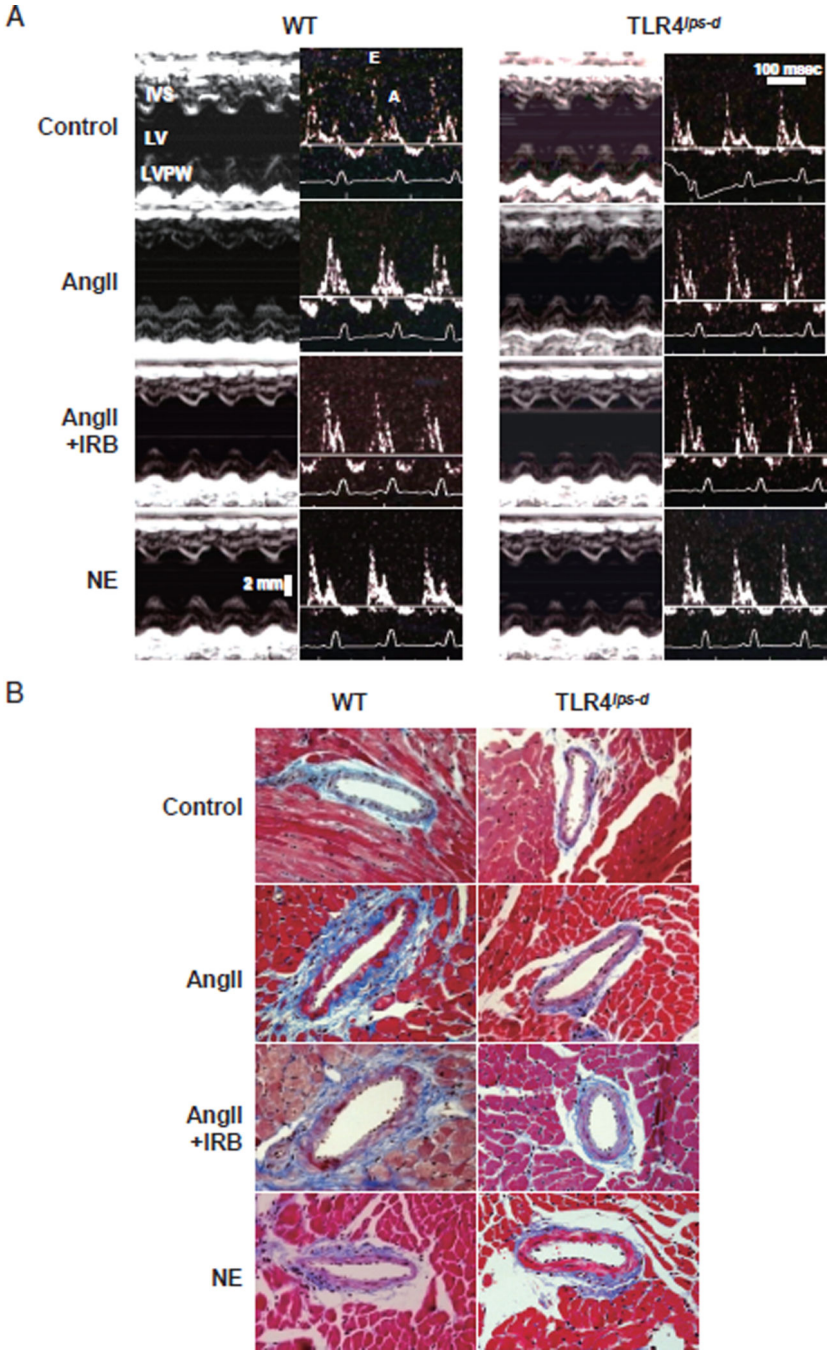

Fig. 1. Representative Echocardiography and Micrographs of Vascular Remodeling and Perivascular Fibrosis in the Intramyocardial Arteries

WT, wild-type mice; TLR4$^{lps\text{-}d}$, TLR4-deficient mice; AngII, angiotensin II; NE, norepinephrine; IRB, irbesartan.

A. Representative echocardiograms of WT and TLR4$^{lps\text{-}d}$ mice. AngII and NE were infused subcutaneously for two weeks using an osmotic mini-pump. The cardiac function was evaluated using transthoracic echocardiography with an ultrasound machine equipped with a 15-MHz probe under light anesthesia and sevoflurane in the WT and TLR4$^{lps\text{-}d}$ mice. Left panel: M-mode recording of the left ventricle. Right panel: transmittal flow assessed on

Doppler echo. IVS, interventricular septum; LV, left ventricle; LVPW, left ventricular posterior wall; E, early ventricular filling wave (E wave); A, late filling wave caused by atrial contractions (A wave). B. Representative micrographs of the effects of TLR4 on vascular remodeling and perivascular fibrosis in the intramyocardial arteries. The sections were stained with Masson Trichrome staining. Bar, 50 μm.

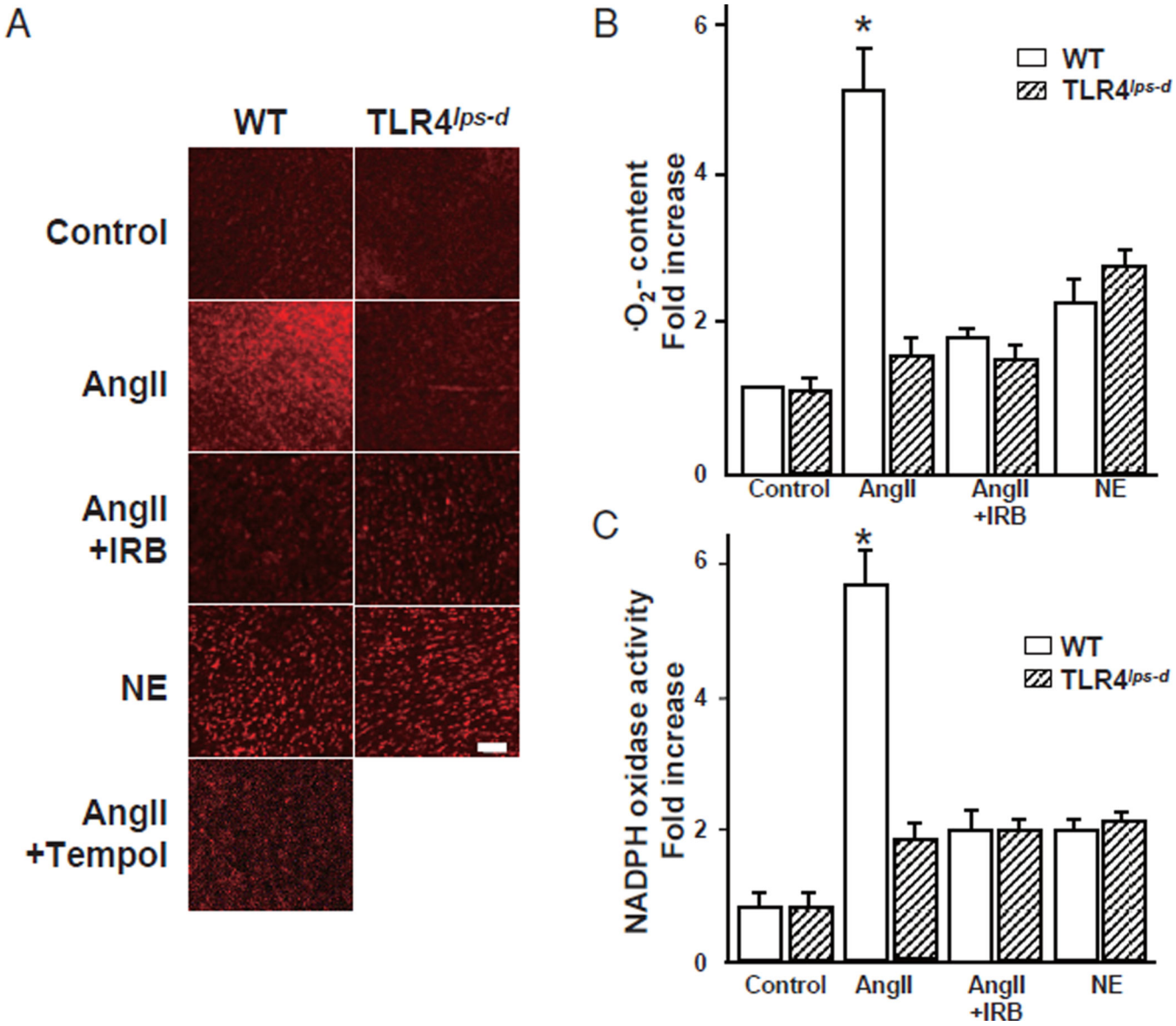

Fig. 2. Reactive oxygen species content and NADPH activity in the heart

WT, wild-type mice; T1r4$^{lps\text{-}d}$, TLR4-deficient mice; AngII, angiotensin II; NE, norepinephrine; IRB, irbesartan.

A. Fluorescent photomicrographs showing the *in situ* detection of $\cdot O_2^-$ in the heart labeled with oxidative dihydroethidium (DHE; red fluorescence). Bar, 100 μm. B. Quantitative analysis of the $\cdot O_2^-$ content. Bar, SE. Experiments, n=3. *p<0.05 vs. the other groups. C. Quantitative analysis of the NADPH oxidase activity using a luminescence assay in the mouse hearts. Bar, SE. Experiments, n= 5. *p< 0.05 vs. the other groups.

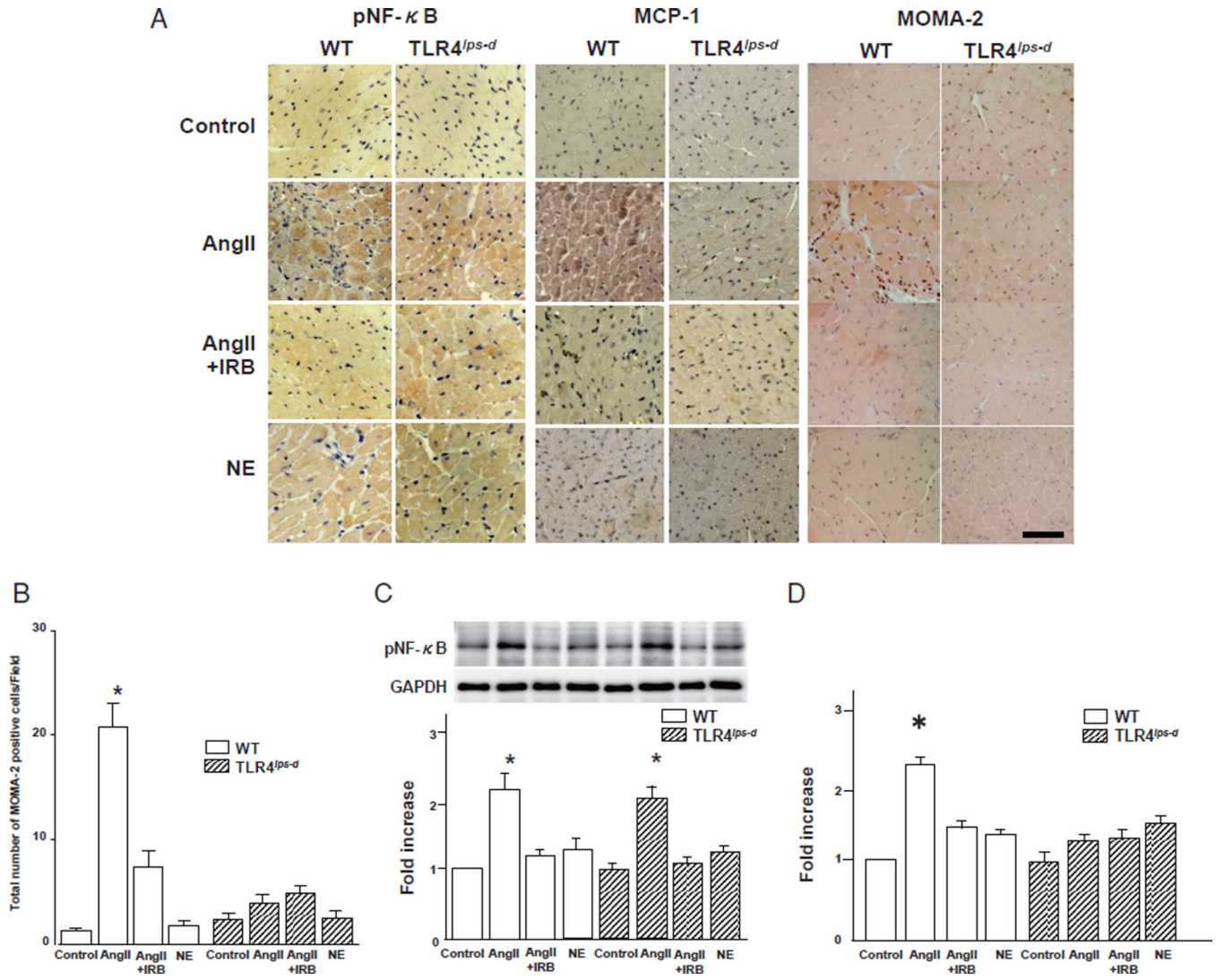

Fig. 3. Expression of pNF-κB and MCP-1 and infiltration of monocytes/macrophages in the heart

WT, wild-type mice; T1r4$^{lps\text{-}d}$, TLR4-deficient mice; AngII, angiotensin II; NE, norepinephrine; IRB, irbesartan.

A. Immunohistochemical staining for pNF-κB and MCP-1 and infiltration of monocytes/macrophages in the mouse heart tissue. pNF-κB stained brown in the cytoplasm and nuclei in the heart. MCP-1 stained brown in the cytoplasm in the heart. Monocytes/macrophages stained brown in the interstitial regions in the heart. MOMA-2; marker of monocytes/macrophages. Bar, 50 μm.

B. Quantitative analysis of the infiltration of monocytes/macrophages in the heart. Bar, SE. Experiments, AngII-treated WT and T1r4$^{lps\text{-}d}$ groups; n= 6, the other groups; n= 3. *P< 0.05 vs. the control, AngII + IRB or NE group in both the WT and T1r4$^{lps\text{-}d}$ mice.

C. Results of a quantitative analysis of the expression of pNF-κB in the heart. Bar, SE. Experiments, n=3. *p<0.05 vs. the control, AngII + IRB or NE group in both the WT and T1r4$^{lps\text{-}d}$ mice. There were no significant differences in the expression of pNF-κB between the WT AngII group and the T1r4$^{lps\text{-}d}$-AngII groups.

D. Quantitative analysis of the expression of MCP-1 in the heart. Bar, SE. Experiments, n = 3. *p<0.05 vs. the other groups.

Table 1

Systolic blood pressure, heart rate, body weight, left ventricular weight/body weight, wall-to-lumen ratio and perivascular fibrosis of the intramyocardial artery

	WT				Tlr4$^{lps\text{-}d}$			
	Control	**AngII**	**AngII + IRB**	**NE**	**Control**	**AngII**	**AngII + IRB**	**NE**
SBP, mmHg	108±5	165±3*	157±1*	158±9*	113±4	173±3*	158±5*	160±7*
HR, bpm	476±37	456±18	507±17	492±19	513±10	425±24	473±23	482±12
BW,g	28.3±0.6	27.3±1.1	27.0±0.8	27.6±0.8	29.0±0.6	30.0±1.7	26.8±0.8	26.9±0.8
LVW/BW, mg/g	4.35±0.1	7.71±0.2*	4.32±0.1	4.81±0.1	4.38±0.2	4.68±0.1	4.71±0.2	4.85±0.1
W/L ratio	0.12±0.003	0.19±0.009*	0.12±0.003	0.14±0.014	0.11±0.003	0.12±0.011	0.11±0.007	0.13±0.009
PVF	0.06±0.005	0.23±0.016$^{\#}$	0.20±0.019	0.09±0.003	0.07±0.004	0.10±0.010	0.14±0.019	0.10±0.006

The values are presented as the mean± SE. Each group, $n = 6$.

$^{*}p<0.05$ vs. the other groups.

$^{\#}p< 0.05$ vs. the other groups, except the AngII+ IRB group in the WT mice.

WT, wild-type mice; Tlr4$^{lps\text{-}d}$, TLR4-deficient mice; AngII, angiotensin II; NE, norepinephrine; IRB, irbesartan; W/L ratio, wall-to-lumen ratio of the intramyocardial arteries; PVF, perivascular fibrosis of the intramyocardial arteries; SBP, systolic blood pressure; HR, heart rate; bpm, beats per minute; BW, body weight; LVW, left ventricular weight.

Table 2

Cardiac parameters assessed using transthoracic echocardiography

	WT				T1r4$^{lps\text{-}d}$			
	Control	**AngII**	**AngII + IRB**	**NE**	**Control**	**AngII**	**AngII + IRB**	**NE**
LVEDd, $\times 10^{-1}$ mm	43.2±0.3	42.3±0.5	39.0±1.2	40.8±0.9	39.3±0.8	40.5±0.9	39.3±0.7	41.8±0.9
LVESd, $\times 10^{-1}$ mm	22.8±0.7	27.8±0.5*	22.8±0.9	24.4±0.8	22.8±0.5	22.8±0.5	23.3±0.3	24.8±0.5
IVSWT, $\times 10^{-1}$ mm	5.5±0.3	9.7±0.3*	6.3±0.3	6.8±0.3	5.3±0.3	5.8±0.3	6.0±0.0	6.3±0.3
PWT, $\times 10^{-1}$ mm	5.0±0.0	9.0±0.6*	7.0±0.6	7.3±0.0	5.0±0.0	6.0±0.0	6.0±0.0	7.0±0.0
%FS, %	50.6±2.7	33.6±1.2*	41.7±1.1	41.0±1.5	43.3±1.7	44.0±1.1	44.2±3.0	40.6±0.3
E/A ratio	2.4±0.2	1.4±0.7*	1.9±0.8	2.0±0.1	2.3±0.2	2.1±0.1	2.3±0.2	2.0±0.1

The values are presented as the mean±SE. Each group, $n = 3$.

*$p<0.05$ vs. the other groups.

WT, wild-type mice; T1r4$^{lps\text{-}d}$, TLR4-deficient mice; AngII, angiotensin II; NE, norepinephrine; IRB, irbesartan; LVEDd, left ventricular end-diastolic dimension; LVESd, left ventricular end-systolic dimension; IVSWT, interventricular septal wall thickness at end-diastole; PWT, posterior wall thickness at end-diastole; %FS, fractional shortening; E/A ratio, early ventricular filling wave (E wave)/late filling wave caused by atrial contractions (A wave) assessed on Echo Doppler.